

Improving the microstructural and physical properties of alumina electrical porcelain with Cr_2O_3 , MnO_2 and ZnO additives

Ž. D. TASIĆ

Institute for Materials (CIRM), "Energoinvest", 71000 Sarajevo, Yugoslavia

The optimum concentrations of Cr_2O_3 , MnO_2 and ZnO were added separately and combined to the basic composition of the alumina electrical porcelain body. The samples were prepared from wet and plastic porcelain bodies according to IEC standard methods. After drying and firing under appropriate conditions, the effects of added oxides on the microstructural and physical properties of sintered porcelain were studied. It was found that the microstructure of this material was remarkably improved compared to one without additives. The sintering temperature was decreased by 60°C , and at the same time closed porosity decreased considerably resulting in a density increase. The mullite content increased slightly, but both the size and shape of its acicular crystals were limited to values providing formation of a very strong network connecting other crystalline phases in the glassy matrix without any significant internal microcracks. It was concluded that these oxides acted as densification catalysts, partly as mineralizers, and as crystal growth inhibitors causing significant improvement of mechanical, electrical and thermal properties of the alumina electrical porcelain investigated.

1. Introduction

Alumina electrical porcelain was developed by replacing quartz with α -alumina in a triaxial porcelain to improve its technical properties [1]. The α -alumina, as a strong thermodynamically stable component, prevents the appearance of internal microcracks in the glassy phase caused by the $\alpha \rightleftharpoons \beta$ inversion of quartz crystals at 573°C , and increases the mechanical strength and thermal shock resistance [2-4]. There are some contradictory views concerning the importance of mullite content in the phase compositions of the sintered porcelain. Khandelwal and Cook [4] and Kato *et al.* [5] found that total mullite content did not affect the strength of porcelain. Palatzky and Tummler [6], Wiedman [7, 8], Grofcsik [9], Kalnin [10], Flaitz and Funk [11] and many other authors have concluded that increasing the mullite content in the porcelain phase composition improved its mechanical properties.

It is known that in the presence of alumina, dissolution of primary mullite in the glassy phase and recrystallization of secondary mullite is suppressed [12]. In attempts to increase the mullite content at lower firing temperature, many experiments were performed by including various substances, as mineralizers, in the compositions of porcelain bodies. For example, AlF_3 [13], TiO_2 and Fe_2O_3 [14, 15] were used in small concentrations as effective mineralizers and their influence on mullitization has been studied. But, in order to achieve extra-high mechanical strength of alumina electrical porcelain (above 200 MPa) it is not sufficient to increase solely the content of alumina and mullite.

It is also necessary to optimize the shape and size of their crystals and to increase the degree of densification by adding various additives acting as crystal growth inhibitors and densification catalysts.

Some authors used talc [16], BaCO_3 [17] and mixes of $\text{TiO}_2 + \text{MnO}_2$ [17, 18] as effective additives and managed to increase the mechanical flexural strength of alumina porcelain to above 200 MPa. Schroeder [19] added small amounts of TiO_2 and ZrSiO_4 as grain growth inhibitors in kyanite porcelain, and MgO , ZnO and $\text{Na}_2\text{ZrSiO}_5$ as very effective densification catalysts.

The inhibitors limited the size of the acicular mullite crystals to $2.0\ \mu\text{m}$ during an appropriate firing cycle. The densification catalysts lowered the viscosity and surface tension of the glassy phase and increased the mobility of atoms at grain boundaries and therefore facilitated the movement of pores out of the material. Both of these effects caused the decrease in closed porosity to under 1.0 vol %, and the increase in mechanical strength to above 210 MPa. According to some opposite views it is not necessary to add any kind of additive, but it is very important to reduce the size of the non-plastic components to less than $10\ \mu\text{m}$, to minimize the free quartz and organic impurities in clay components and to adjust the firing conditions [11, 20, 21].

The objective of the present work was to research the effects of Cr_2O_3 , ZnO and MnO_2 additives on the microstructural and technical properties of alumina electrical porcelain with the intention to improve them as much as possible. The main reasons for the choice

of these oxides were the following: in the available literature there were few data concerning their individual application as catalysts or mineralizers in an electrical porcelain body. Their effects on the porcelain in combination with other oxides or complex compounds have been studied more often [17–19]. Also, it is known that a small amount of Cr_2O_3 increases the mechanical strength of corundum–mullite ceramics by the formation of $(\text{Al}, \text{Cr})_2\text{O}_3$ solid solution, but the effects of Cr_2O_3 on the electrical alumina-porcelain were not known. It was thought that it would be interesting and useful to research individual effects of the chosen oxides on this ceramic because their bond strength and coordination numbers allow them to enter the structure of aluminosilicate glass and to change its properties significantly. The effects of these combined oxides have also been studied in order to compare the results obtained. Optimum concentrations (up to 2.0 wt %) of chosen oxides were added separately and combined to the basic composition of the porcelain body instead of the same amounts of feldspar.

The samples were prepared by the wet forming method, and after drying and firing, the physical properties were examined by applying the methods in accordance with IEC standard. Qualitative and quantitative crystal phase composition of the fired porcelain samples were determined by X-ray diffraction analysis.

The microstructure was examined using scanning electron microscopy (SEM).

2. Experimental procedure

2.1. Raw materials

The experimental compositions of the porcelain

bodies were prepared from the following raw materials: Alumina, feldspar, ball clays I and II, and kaolin. Their mineralogical and chemical compositions are presented in Tables I and II.

As special additives, the following were chosen: manganic oxide (MnO_2), chromic oxide (Cr_2O_3) and zinc oxide (ZnO).

2.2. Preparation of raw samples

On the basis of mineralogical and physico-chemical properties of the raw materials, the basic composition of the porcelain body (C-0) was estimated without any additives. Four compositions (C-1, C-2, C-3 and C-4) were obtained by including in the basic compositions 1.5% Cr_2O_3 , 1.0% MnO_2 , 2.0% ZnO and (0.5% Cr_2O_3 + 0.5% MnO_2 + 0.5% ZnO), respectively, instead of the same amounts of feldspar. The starting compositions of the experimental electrical porcelain bodies are presented in Table III.

All experimental mixtures were prepared by mixing finely ground components as a water suspension (slurry). In order to achieve the optimum homogeneity and particle size distribution of the slurries, the additional 10 h milling were performed in a laboratory ball mill. The viscosity and bulk density were adjusted to the optimum values: 3–5 Pas, and 1.45–1.50 Mg m^{-3} . The viscosity was measured using a Brookfield's rotating viscometer (model RVF, USA). The particle size distribution of basic composition (C-0) was determined before and after additional milling (Fig. 1) using a sedimentary balance, "Prolabo" (France).

After removal of excess water from the slurries by filter pressing, the wet plastic bodies were extruded on the laboratory vacuum press to obtain samples for determination of optimum sintering temperature and

TABLE I Mineralogical composition of the raw materials (wt %)

Component	Ball clay I	Ball clay II	Kaolin	Alumina	Feldspar
Kaolinite	64.0	75.0	78.0		
Illite	8.0	8.0			
Montmorillonite	17.0				
Muscovite			18.0		
Quartz	8.0	14.0	2.5		4.0
Orthoclase					65.3
Albite					27.2
α -alumina				98.0	
Minor minerals ^a	3.0	3.0	1.5	2.0	3.5

^a Haematite, rutile, calcite, magnesite and γ - Al_2O_3 .

TABLE II Chemical compositions of the raw materials (wt %)

Oxide	Ball clay I	Ball clay II	Kaolin	Alumina	Feldspar
SiO_2	57.28	57.56	47.47	0.11	66.66
Al_2O_3	27.26	28.20	36.97	99.33	18.57
TiO_2	1.32	1.58	0.06		
Fe_2O_3	2.34	0.92	0.91	0.14	0.35
CaO	0.49	0.32	0.12	0.07	0.17
MgO	0.48	0.32	0.25		
K_2O	0.52	0.42	1.62		10.45
Na_2O	0.11	0.10	0.11	0.18	3.05
L.O.I.	10.20	10.58	12.40	0.16	0.17

TABLE III Starting compositions of the experimental electrical porcelain bodies (wt %)

Raw material	C-0	C-1	C-2	C-3	C-4
Alumina	45.0	45.0	45.0	45.0	45.0
Feldspar	21.0	19.5	20.0	19.0	19.5
Kaolin	9.0	9.0	9.0	9.0	9.0
Ball clay I	16.0	16.0	16.0	16.0	16.0
Ball clay II	9.0	9.0	9.0	9.0	9.0
Cr ₂ O ₃		1.5			0.5
MnO ₂			1.0		0.5
ZnO				2.0	0.5

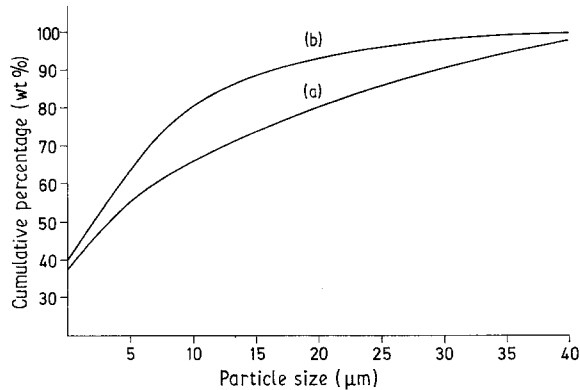


Figure 1 Particle size distribution of basic raw composition, (a) before additional milling, (b) after additional milling.

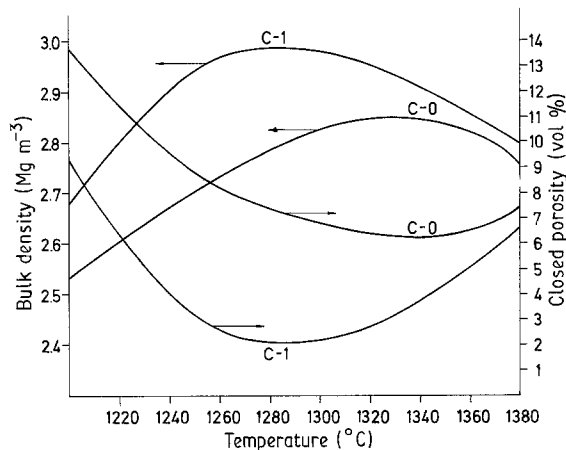


Figure 2 Change of bulk density and closed porosity of electrical porcelains C-0 and C-1 with increasing temperature.

for investigation of physical properties according to IEC standard. Then they were dried at room temperature for 48 h and at 110 °C in a laboratory electrical drier for a further 6 h.

2.3. Determination of optimum sintering temperatures and firing cycles

The porcelain samples of all body compositions were heated after being dried in the laboratory gas furnace (Bicley, USA). To determine the optimum sintering temperatures, firing of samples was performed at ten different temperatures in the range 1200–1380 °C in an oxidizing–reducing atmosphere. The final temperature of each firing was increased by 20 °C. The holding time at the final temperatures was 120 min and total time of the firing cycle was 48 h.

The linear shrinkage, water absorption (open porosity), bulk density and true density were measured by the usual standard methods. The percentage of closed porosity was calculated from the bulk density/true density ratio. The values of these physical properties were tabulated and plotted as functions of increasing temperature. The optimum sintering temperature is that at which the linear shrinkage and bulk density attain maximum values, while the water absorption and closed porosity attain minimum values. From these parameters it can be seen that an optimum sintering temperature of C-0 porcelain composition, without any additives is 1340 °C and that the optimum sintering temperature of the other porcelain compositions with additives is 1280 °C. The changes in these values depend on increasing temperature, and are presented in Table IV and Figs 2 and 3 only for C-0 and C-1 porcelain compositions, because of the greater difference between them than between C-0 and the others.

Based on the optimum sintering temperatures the exact firing cycles were determined (Fig. 4) with following parameters: firing time (cold-cold), 50 h; final firing temperature for C-0, 1340 °C; final firing temperature for C-1, C-2, C-3, C-4, 1280 °C; holding time, 90 min; firing atmosphere, oxidizing–reducing. The porcelain standard samples fired according to these cycles were subjected to the determination of physical and microstructural properties.

TABLE IV Linear shrinkage, bulk density, water absorption and closed porosity of fired of C-0 and C-1 samples

Temperature T(°C)	Linear shrinkage (%)		Bulk density (Mg m ⁻³)		Water absorption (wt %)		Closed porosity (vol %)	
	C-0	C-1	C-0	C-1	C-0	C-1	C-0	C-1
1200	5.6	8.8	2.51	2.68	5.6	4.8	13.7	9.2
1220	6.9	10.6	2.58	2.79	3.7	2.5	11.5	6.2
1240	8.2	12.4	2.67	2.84	2.9	1.0	9.6	4.0
1260	9.6	13.8	2.70	2.89	1.3	0.0	8.5	2.5
1280	10.9	14.0	2.75	2.93	0.4	0.0	7.4	2.3
1300	11.6	13.9	2.78	2.92	0.2	0.0	6.9	2.4
1320	11.9	13.5	2.81	2.87	0.0	0.1	6.4	2.6
1340	12.0	12.8	2.82	2.83	0.0	0.5	6.2	3.4
1360	11.9	11.9	2.80	2.79	0.0	0.9	6.5	4.8
1380	11.2	10.2	2.76	2.72	0.5	1.4	7.3	6.7

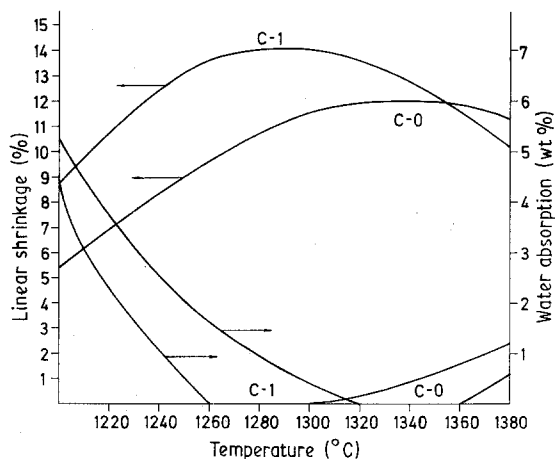


Figure 3 Change of linear shrinkage and water absorption of electrical porcelain C-0 and C-1 with increasing temperature.

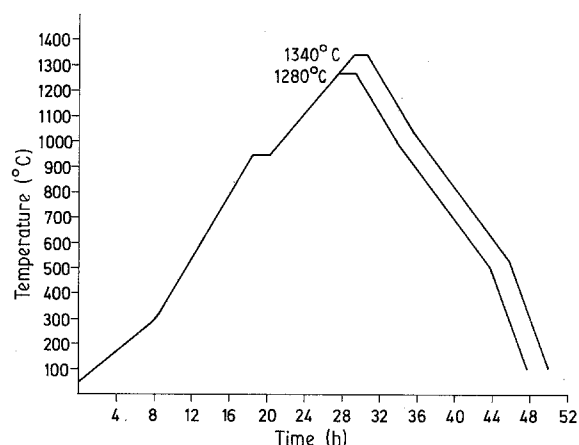


Figure 4 Temperature firing cycles of the experimental electrical porcelain bodies.

TABLE V Values of physical properties of experimental electrical porcelains compared to IEC standard values

Properties	symbol	units	IEC-672-3 1984							
			C-100	130	C-0	C-1	C-2	C-3	C-4	
Open porosity:	max.,	P_a	(vol %)	0.0	0.0	0.0	0.0	0.0	0.0	0.0
Bulk density:	min.,	ρ_a	(Mg m ⁻³)	2.5	2.85	2.98	2.92	2.86	2.96	2.96
Flexural strength										
Unglazed:	min.,	R_f	(MPa)	140	184	242	224	218	232	232
Glazed:	min.,	R_g	(MPa)	160	207	285	266	256	273	273
Modulus of elasticity:	min.,	E	(GPa)	100	143	163	156	146	159	159
Mean coefficient of thermal expansion										
20–300°C:		α	(10 ⁻⁶ K ⁻¹)	4–7	4.2	4.0	4.0	4.1	4.0	4.0
20–600°C:		α	(10 ⁻⁶ K ⁻¹)	4–7	5.0	5.0	5.2	5.2	5.3	5.3
20–1000°C:		α	(10 ⁻⁶ K ⁻¹)	5–7	5.2	5.7	5.7	5.7	5.8	5.8
Resistance to thermal shock:	min.,	Δt	(K)	150	170	200	200	200	200	200
Electric strength:	min.,	E_d	(kV mm ⁻¹)	20	23	29	28	26	30	30
Withstand voltage:	min.,	U	(kV)	30	39	45	44	43	44	44
Dissipation factor; 50 Hz, 23°C:	max.,	$\tan \delta$	(10 ⁻³)	30	19.4	15.6	17.2	18.7	15.9	15.9
Dielectric constant; 50 Hz, 23°C:		ϵ_r		6–7.5	7.0	7.0	6.8	7.0	6.9	6.9
Volume resistivity; 23°C:	min.,	ρ_v	(10 ¹² Ω)cm	10	77	160	130	92	140	140

2.4. Determination of physical and microstructural properties and results

The determination of most important physical properties of fired porcelain samples was performed by methods in accordance with standard IEC publication 672–3, 1984, C-100, 130.

The open porosity and bulk density were determined by boiling test and using Jolly hydrostatic balance (Welch, USA). The mechanical strength was measured on bars of 120 mm length and 10 mm diameter by a three-point bending (flexural) test using a laboratory testing machine (Mohr and Federhaff, Germany).

The modulus of elasticity was determined by a dynamic method with ultrasonic resonance frequency measurement using an ultrasonic apparatus. (UDP-2 type NE228 Iskra, Yugoslavia). The mean coefficient of linear thermal expansion was measured on the samples of 50 mm length and 4 mm diameter using a dilatometer of type Linseis at a heating rate of 5°C min⁻¹ up to 1000°C.

The resistance to thermal shock was examined by a visual cracking test on the fired samples of the same

form and size as the samples used for determination of mechanical strength, by heating and cooling them alternately. The electrical strength and withstand voltage were measured using a high-voltage transformer of 100 kV and kVA (Energoinvest, Yugoslavia).

The dissipation factor and dielectric constant were measured using a Schering bridge at 50 Hz and 23°C (type 2801, Tettex, Switzerland), and for determination of the volume resistivity, a Multi Megohm-meter (type MOM11, WTV, Germany) was used.

The average results of the measurements of these physical properties are presented in Table V. Table VI shows the good correlation between the flexural strength, bulk density and closed porosity. Using the values from this table Fig. 5 was drawn showing the increase in flexural strength of porcelains with additives, depending on decreasing closed porosity.

The main crystal phases of the fired porcelain samples were identified by X-ray diffraction (XRD) analyses using a diffractometer with CuK_α radiation (type Philips PW 1051). Quantitative phase analyses were made using CaF₂ as an internal standard. The amount of amorphous phase was estimated as the difference

TABLE VI Mechanical strength, strength increase, bulk density and closed porosity of experimental porcelains

Type of porcelain	Flexural strength (MPa)		Strength increase (%)		Bulk density (Mg m ⁻³)	Closed porosity (vol %)
	Unglazed, R _f	Glazed, R _g	R _f	R _g		
IEC 672-3						
C-100 130	140.0	160.0			2.50	
C-0	174.0	207.0	24.3	29.4	2.85	6.2
C-1	242.0	285.0	72.8	78.0	2.99	1.7
C-2	224.0	266.0	60.0	66.2	2.92	3.2
C-3	218.0	256.0	55.7	60.0	2.86	4.3
C-4	232.0	273.0	67.5	70.0	2.96	2.6

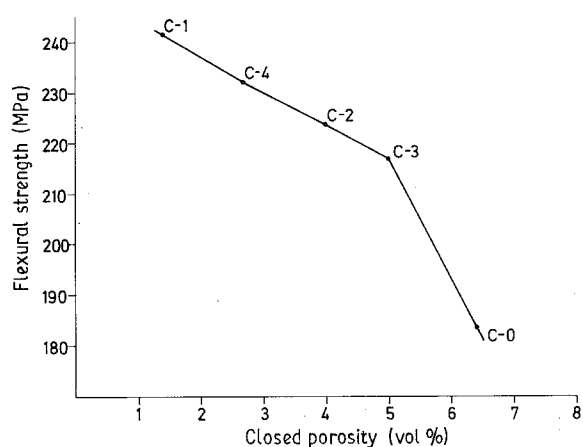


Figure 5 Increasing flexural strength with decreasing closed porosity of experimental electrical porcelains under the influence of additives.

from 100%. The results of qualitative crystal phase analyses are shown as diffractograms in Fig. 6, and the results of quantitative phase analyses are given in Table VII.

The microstructure of experimental electrical porcelains was investigated using scanning electron microscopy (SEM, type Jeol 35C) with fractured fired samples etched in 10% HF. Micrographs are presented in Fig. 7.

3. Discussion

The results have shown that added oxides have a great influence on the physical and microstructural properties of the investigated electrical porcelain produced under proper conditions. They lowered its optimum sintering temperature by 60 °C, significantly increasing the bulk density and decreasing closed porosity at the same time (Table IV).

From Table V it can be seen that almost all physical properties of porcelains with additives are much better than those of the porcelain (C-0) without additives, in relation to the IEC standard values. The flexural strength increase of unglazed porcelain sample (C-0) is only 24.3%, while the increases in flexural strength of unglazed porcelain samples with additives Cr₂O₃ (C-1), MnO₂ (C-2), ZnO (C-3) and Cr₂O₃ + MnO₂ + ZnO (C-4) are 72.8%, 60.0%, 55.7% and 67.5%,

respectively. The increase in strength of the glazed samples is up to 78.0%.

From Table VI good correlation can be observed between the bulk density or the closed porosity with mechanical strength. Fig. 5 shows the change in flexural strength as a function of the closed porosity, which is opposite to the result mentioned by Khandelwal and Cook [4]. The influence of added oxides could be partly explained by their action as densification catalysts.

All standard porcelains have no open porosity after regular firing, but they always contain a considerable numbers of closed pores (6–10 vol %). The content of closed pores in porcelain sample C-0 is 6.2 vol %, because of the high viscosity and, consequently, the low atom mobility in the large amount of aluminosilicate melt which is created (30–40 wt %) at the maximum firing temperature of porcelain by chemical combination of fluxing components with alumina and silica. It is supposed that in this kind of liquid phase most of the atom movement necessary for pore movement is concentrated along grain boundaries. In this case a high degree of densification cannot be achieved because at the cooling temperature the pores will be trapped inside the glassy phase or the grain boundary and will be unable to migrate to the surface. The presence of closed pores in the porcelain reduces its mechanical strength because the pores act as a brittle phase of zero strength.

Small amounts of added oxides acting as densification catalysts decrease the melting point of the flux (K-Feldspar) by 100–150 °C approximately, and lower the viscosity and surface tension of the glassy melt in grain-boundary zones at the maximum firing temperature. The atom mobility is increased facilitating movement of the pores towards the surface and out of the sintering porcelain, thus increasing its density [19]. According to Grimshaw [22], in the final stage of sintering, densification proceeds by the removal of closed pores by grain growth, but mainly in the presence of a small amount of liquid phase. In that case a contact between the solid grains and liquid phase depends on surface tension forces and the degree of wetting. The degree of wetting is defined as the contact angle (dihedral angle) between the liquid phase and solid grains. During vitrification in ceramic bodies, with the contact angle lower, the liquid will

TABLE VII Phase composition of the investigated electrical porcelains (wt %)

Porcelain	Mullite	Corundum	Quartz	Gahnite	Amorphous phase
C-0	12.4	43.8	2.3		41.5
C-1	14.4	44.2	2.2		39.2
C-2	13.2	44.3	2.4		40.1
C-3	15.4	43.7	2.2	4.0	34.7
C-4	13.5	44.2	2.3	2.0	38.0

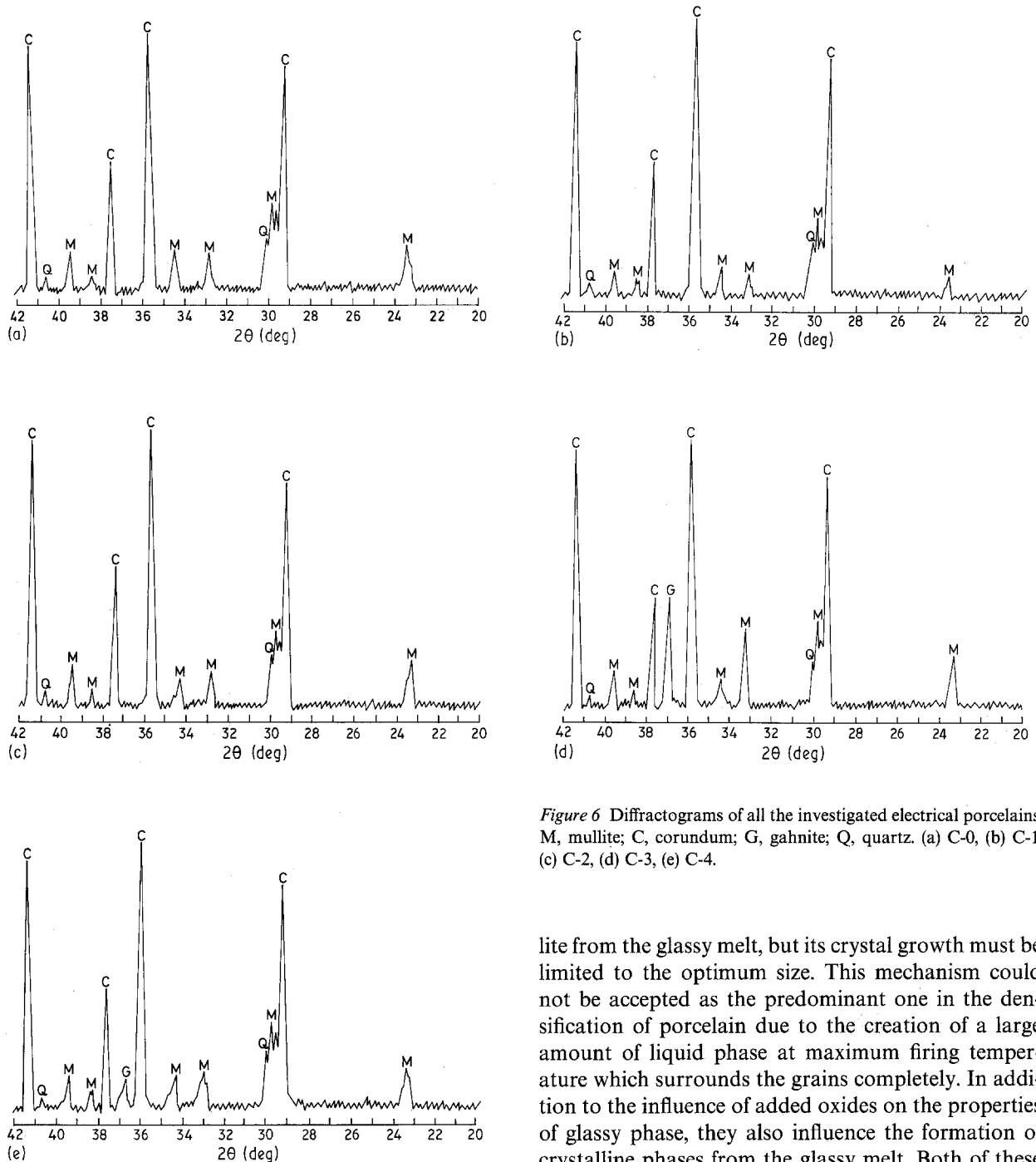


Figure 6 Diffractograms of all the investigated electrical porcelains. M, mullite; C, corundum; G, gahnite; Q, quartz. (a) C-0, (b) C-1, (c) C-2, (d) C-3, (e) C-4.

lite from the glassy melt, but its crystal growth must be limited to the optimum size. This mechanism could not be accepted as the predominant one in the densification of porcelain due to the creation of a large amount of liquid phase at maximum firing temperature which surrounds the grains completely. In addition to the influence of added oxides on the properties of glassy phase, they also influence the formation of crystalline phases from the glassy melt. Both of these processes affect the densification of porcelain.

Diffractograms of qualitative X-ray analyses (Fig. 6) have shown that porcelains of C-0, C-1 and C-2 compositions contain corundum ($\alpha\text{-Al}_2\text{O}_3$) and mullite ($3\text{Al}_2\text{O}_3 \cdot 2\text{SiO}_2$) as crystal constituents and quartz ($\alpha\text{-SiO}_2$) as a residual ingredient from clay components and feldspar. The porcelain of C-3 and C-4 compositions in addition to the aforementioned minerals, also contain mineral gahnite (ZnAl_2O_4).

make contact with or wet the solid grains more readily, enhancing their growth. Addition of small amounts of some metal oxides, especially Cr_2O_3 , produces a liquid phase of low contact angle which increases the crystal grains.

In porcelain densification, this mechanism might be partly related to the crystallization of secondary mul-

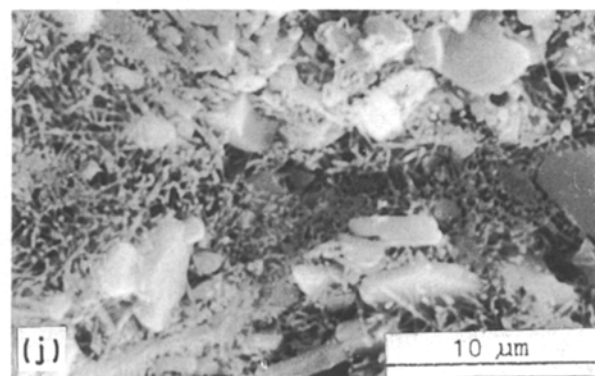
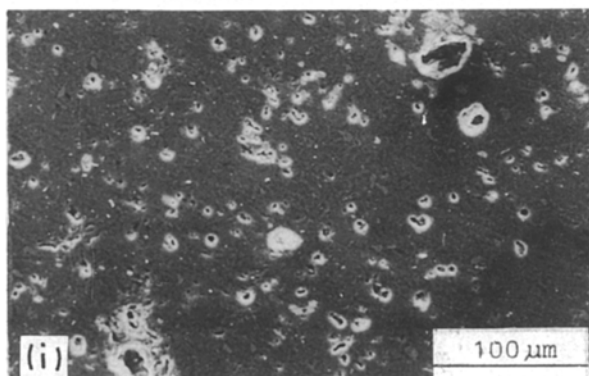
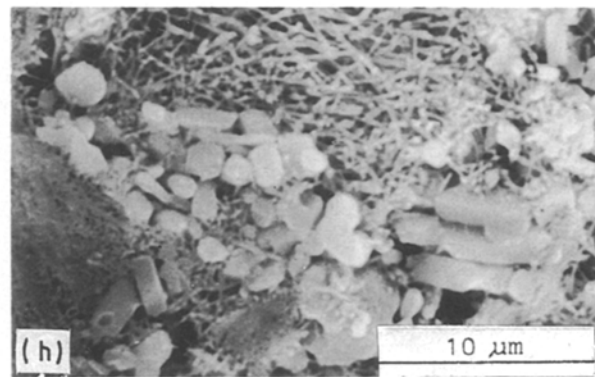
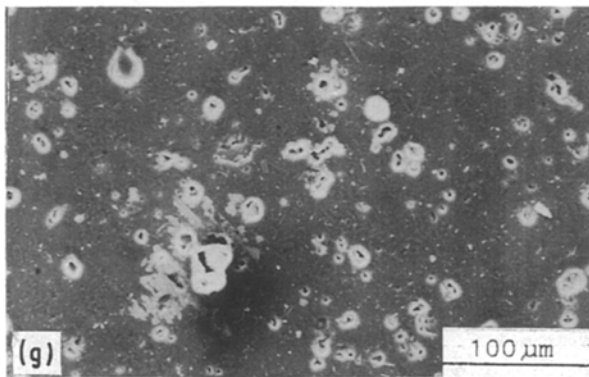
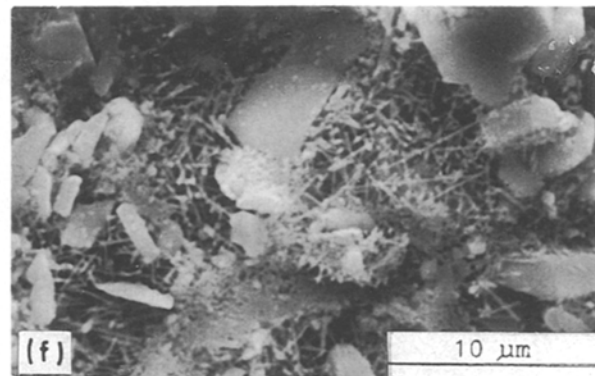
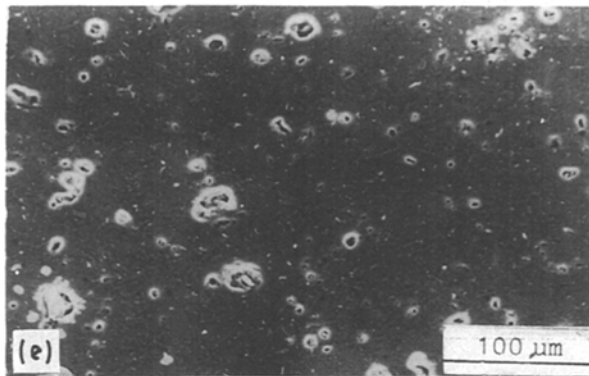
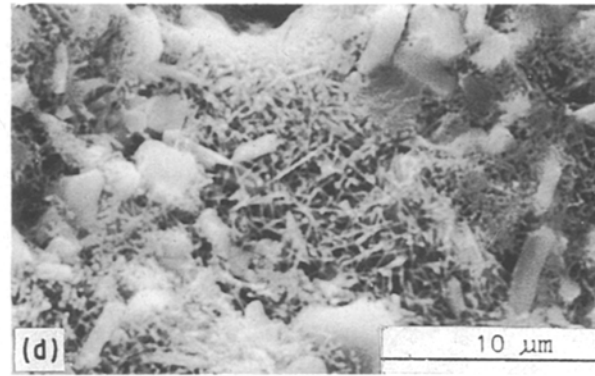
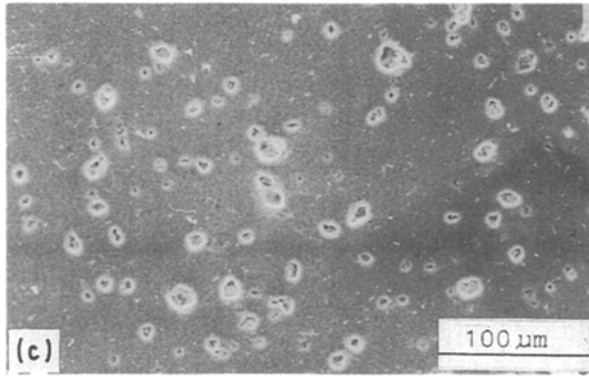
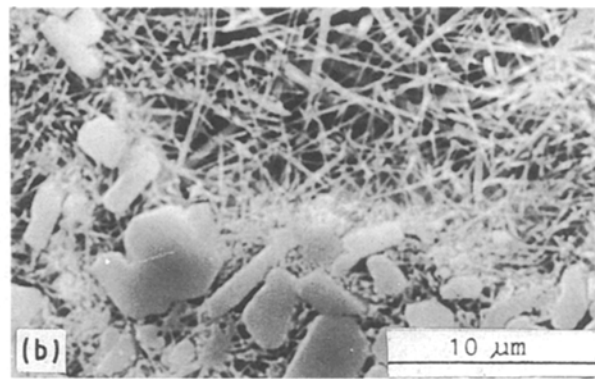
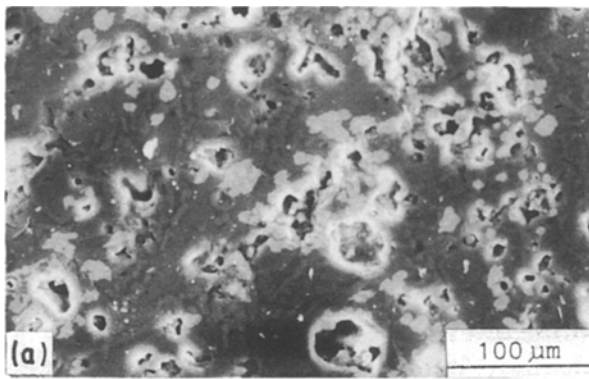


Figure 7 Scanning electron micrographs of all the investigated electrical porcelains: (a, c, e, g, i) showing the pores, (b, d, f, h, j) showing crystalline constituents. (a, b) C-0, (c, d) C-1, (e, f) C-2, (g, h) C-3, (i, j) C-4.

Results of quantitative X-ray phase analyses presented in Table VII have shown that porcelain samples with additives contain more mullite than porcelain samples (C-0) without additives. The added oxides promoting early formation of liquid phase influence the kinetics of the formation of new crystal phases and earlier dissolution of Al_2O_3 and SiO_2 from decomposed clay minerals and residual of quartz. It is probable that these additives accelerate the exothermic process of mullitization at lower temperature than is usual, due to the decrease in activation energy of clay mineral decomposition. However, the total content of mullite thus formed is considerably lower than the theoretical one. This is in good conformity with Shuller's [12] conclusion that the formation and dissolution of mullite is suppressed by the presence of fine $\alpha\text{-Al}_2\text{O}_3$ in the glassy phase. There is insufficient proof that increasing the mullite content is the main factor affecting the improvement of mechanical or any other properties of alumina electrical porcelain. It is in disagreement with data presented by Flaitz and Funk [11].

From Table VII it can be seen that porcelain (C-3) with ZnO as an additive has the biggest content of mullite of all, but almost all physical properties of this porcelain sample are weaker than the others containing additives (Table V). Corundum grains of average size $8.0\ \mu\text{m}$ are the inactive phase and their amount is slightly decreased by dissolution in a glassy melt at the maximum sintering temperature.

The presence of free quartz in amounts of $\sim 2.0\ \text{wt}\%$ should be reduced as much as possible because it has a negative influence on the mechanical strength.

By comparing the scanning electron micrographs of the investigated porcelain samples (Fig. 7) an essential difference can be seen in the type of microstructure between alumina electrical porcelains with and without additives. The porcelain sample of C-0 composition is more porous. The pore shape is round and oval, more or less deformed, with a diameter up to $30\ \mu\text{m}$, approximately. Many of them are mutually connected, thus forming channels of irregular shape. On the surface of the cross-section of the sample it can be noticed that internal pores are unevenly dispersed in the glassy phase (Fig. 7a).

By analysing the crystal phase of the same sample (Fig. 7b) one can see that both types of mullite crystal are formed. The primary type of mullite has a shape of compact aggregates of small seeds. Secondary mullite has a shape of acicular crystals of the length up to $15\ \mu\text{m}$, approximately. The crystals of this size are not closely connected with alumina particles. It was found that acicular mullite crystals longer than $5\ \mu\text{m}$ increase interspaces and pores inside the glassy phase inducing weak mechanical strength and other properties.

The samples of porcelain containing additives have lower numbers of internal pores. The shape of these pores is again round and elliptical, but the average diameter is only $5.0\ \mu\text{m}$ and their distribution in the glassy phase is more even (Fig. 7c).

A comparison of the mullite phase in these porcelains shows that secondary mullite crystals are very

different in size and distribution. The structure of electrical porcelain doped with chosen oxides contains smaller acicular mullite crystals – up to only $5.0\ \mu\text{m}$ (Fig. 7d), because the added oxides are somewhat fluxing in their densification action and can limit crystal growth to the optimum size distribution under the approximate firing cycle. Such mullite crystals are interlaced in all directions forming a space network of closely connecting corundum grains throughout the glassy phase without any significant structural defects. This indicates that the shape and size of mullite crystals are more important for the improvement of porcelain properties than is their total amount.

A certain difference can be noticed also in the microstructures and physical properties of the porcelains doped with additives. Each of these additives has a particular influence on the thermochemical reactions causing a certain difference in the phase composition, grain growth and densification process. It was impossible to determine equilibrium conditions and the composition of the porcelain liquid phase due to the high complexity of the porcelain polycomponent system. However, it is most probable that dissolution of $\gamma\text{-Al}_2\text{O}_3$ from decomposed clay minerals in the liquid melt of porcelain sample C-3, is followed by a decrease in the ZnO concentration, partly forming the mineral gahnite, (Fig. 6d). Crystallization of this mineral from the glassy melt increased the content and size of interspaces and pores in sintered porcelain C-3. It caused lower values of physical and microstructural properties than those which have the porcelains containing Cr_2O_3 and MnO_2 additives, despite the greater mullite content as mentioned above.

By analysing the diffractograms and micrographs of samples C-1 and C-2, it was not found that oxides Cr_2O_3 and MnO_2 participate in crystallization of any new minerals.

Energy dispersive spectroscopy (EDS) analysis has shown the presence of chromium and manganese ions only in the glassy phase. Definite crystalline modifications in which additives take part are difficult to identify because of their small amounts and probably as they easily form solid solutions in the presence of liquid phase. Based on the hypothesis of the sub-microstructure of the glassy phase, it might be supposed that a small part of Al_2O_3 after dissolution in the glassy melt may come into contact with Cr^{3+} and Mn^{2+} ions forming cryptocrystalline solid solutions or spinels of defect lattice and becoming finely divided in the glassy matrix. They strengthen the cementing bond of the liquid phase which joins the other crystal grains together more firmly than one containing gahnite (ZnAl_2O_4).

From the obtained results it can be seen that the Cr_2O_3 additive has the best efficiency. Alumina porcelain doped with $1.5\ \text{wt}\%$ Cr_2O_3 after firing in a reducing atmosphere above 1000°C with CO as reducer, has a specific light-violet colour and better physical and microstructural properties than porcelain doped with MnO_2 and ZnO additives under the same conditions. It is supposed that the reason for that is the presence of $(\text{Al}, \text{Cr})_2\text{O}_3$ solid solution finely

divided in the glassy phase, strengthening it somewhat more than other oxides.

The term "catalysts" for added oxides is not strictly applicable, although they greatly accelerate the transformation of glassy phase and induce mullitization to a certain extent, but they react chemically to form the final product from which they cannot be excluded and restored to their initial stage.

A more precise explanation of the action of Cr_2O_3 and MnO_2 on the complex system of alumina porcelain is the subject of further research using more adequate technical methods.

4. Conclusions

Based on the results and observations presented in their work it can be concluded that chosen oxides added in optimum concentrations to the basic raw composition of an electrical porcelain body with adjusted grain size distribution, and under optimum firing conditions, produced the following effects.

1. They lower the temperature of sintering, by 60 °C, reducing consumption of energy;

2. They partly act as mineralizers, increasing the content of mullite by 2%–3% only, so that the total amount is significantly below the theoretical one.

3. They act as crystal growth inhibitors limiting the size of secondary mullite crystals to 5 μm during the holding time at the final firing temperature. This indicates that shape and size of mullite crystals are more important for the improvement of technical properties of electrical porcelain than is their total amount.

4. By acting as densification catalysts they increase density and decrease porosity, enabling the formation of more compact and homogeneous microstructure of sintered electrical porcelain.

All these effects resulted in a significant improvement of technical properties of this ceramic material.

Results of this work are of the great significance for producing the extra-high-strength electrical porcelain, especially by the porcelain body composition C-1 containing 1.5 wt % Cr_2O_3 additive. This ceramic material is very applicable for the production of high-tension insulators of highest technical requirements for apparatus of special construction and function.

Acknowledgements

The author thanks the Institute for Materials (CIRM) and the Energoinvest's Electrical porcelain factory in Sarajevo, for financial support and technical assistance in preparation and investigation of test specimens.

References

1. J. R. FLOYD, J. H. STERNE III and J. S. DEUTSCHER, *Ceram. Age* **82** (1966) 60.
2. B. E. WAYE, M. ASHLEY, B. GIBSON, B. HALES and G. JAMES, *Trans. Brit. Ceram. Soc.* **62** (1963) 421.
3. S. I. WARSHAV and R. J. SEIDER, *Amer. Ceram. Soc. Bull.* **50** (1967) 337.
4. S. K. KHANDELWAL and R. I. COOK, *Amer. Ceram. Soc. Bull.* **49** (1970) 522.
5. S. KATO, T. YAMAMOTO, T. HATTORI and Y. NISHIMURA, *Nagoya Kogyo Gijutsu Shikensho Hokoky* **14** (1965) 355.
6. A. PALATZKY and W. TUMMLER, *Silikat Tech.* **9** (1958) 68.
7. T. WIEDMANN, *Sprechsaal* **92** (1959) 29.
8. *Idem, ibid.* **92** (1959) 52.
9. J. GROFCSIK, *Epitoanyag.* **18** (1966) 197.
10. I. L. KALNIN, *Amer. Ceram. Soc. Bull.* **46** (1967) 1174.
11. P. L. FLAITZ and J. E. FUNK, in "The Effect of Mullite on the strength of High Alumina Electrical Porcelain" (Alfred University, Alfred, NY, 1977) pp 41–8.
12. K. H. SCHULLER, *Trans. J. Brit. Ceram. Soc.* **63** (1964) 103.
13. B. P. LOCSEI, *Interceram.* **3** (1968) 237.
14. H. E. SCHWIERE and C. ZOGRAFOU, *Ber. Dt. Keram Ges.* **47** (1970) 471.
15. S. P. CHAUDHURI, *Amer. Ceram. Soc. Bull.* **53** (1974) 169.
16. E. M. SALLAM and H. W. HENICKE, *Trans. J. Brit. Ceram. Soc.* **82** (1983) 102.
17. ROSENTHAL TECHNIC AG, BRD, Pat. DE 2932914 C2 (1984).
18. H. SHUBERT and D. WETZLAR, *Sprechsaal* **121** (1988) 921.
19. J. E. SCHROEDER, *Amer. Ceram. Soc. Bull.* **57** (1978) 526.
20. J. E. FUNK and I. O. KNICKERBOCKER, *US Pat.* 4183, 760 (1980).
21. S. W. STEERE and J. E. FUNK, *Amer. Ceram. Soc. Bull.* **65** (1986) 1415.
22. R. W. GRIMSHAW, "The Chemistry and Physics of Clays and Allied Ceramic Materials" (Benn, London, 1971) p. 685

Received 3 June 1991

and accepted 1 May 1992